ELEMENTA
Science of the Anthropocene

Abeed, R, et al. 2021. A space view of agricultural and industrial changes during the Syrian civil war. *Elem Sci Anth*, 9: 1. DOI: https://doi.org/10.1525/elementa.2021.000041

RESEARCH ARTICLE

A space view of agricultural and industrial changes during the Syrian civil war

Rimal Abeed[1,*], Cathy Clerbaux[1,2], Lieven Clarisse[2], Martin Van Damme[2], Pierre-François Coheur[2], and Sarah Safieddine[1]

The agricultural sector in Syria was heavily affected by the civil war that started in 2011. We investigate the war's impact on the country's atmospheric ammonia (NH_3) from 2008 to 2019, using measurements from the infrared atmospheric sounding interferometer instrument on board the Metop satellites. We examine the changes in NH_3 close to a fertilizer industry, whose activities were suspended due to conflict-related events. We also explore the effect of war-induced land use/land cover changes on agriculture-emitted ammonia in north-east Syria that has witnessed battles between different groups. The interpretation of the changes in NH_3 is supported by different datasets: visible satellite imagery to assess the effect on industrial activity, reanalysis data from the European center for medium-range weather forecasts to look at the effect of meteorology (temperature, wind speed, and precipitation), and land cover and burned area products from the moderate resolution imaging spectroradiometer (MODIS) to examine land use/land cover changes and fire events during the study period. We show that the NH_3 columns are directly affected by the war. Periods of intense conflict are reflected in lower values over the industry reaching –17%, –47%, and –32% in 2013, 2014, and 2016, respectively, compared to the [2008–2012] average, and a decrease reaching –14% and –15% in the croplands' area in northeast Syria during 2017 and 2018 (compared to 2011), respectively. Toward the end of the control of Islamic State in Iraq and Syria, an increase in atmospheric NH_3 was accompanied by an increase in croplands' area that reached up to +35% in 2019 as compared to prewar (2011). This study shows the relevance of remote-sensing data of atmospheric composition in studying societal changes at a local and regional scale.

Keywords: Ammonia, Agriculture, Syria, Remote sensing, IASI, Satellite

1. Introduction

The Syrian civil war started in March 2011 and caused dramatic social, political, economic, and environmental consequences over the whole country. Agriculture suffered massively, which also affected the economy directly since the agricultural sector makes up to 26% of the gross domestic product (FAO, 2017a). Several studies used satellite-retrieved data and/or imagery to examine the changes in the region during the conflict (Corbane et al., 2016; Jaafar and Woertz, 2016; Eklund et al., 2017; Dammers et al., 2019; Mohamed et al., 2020). The crisis caused a massive displacement of refugees, inside Syria and to other countries. A total of 13.2 million individuals were displaced. This includes 6.6 million refugees outside of Syria and more than 6 million internally displaced (UNHCR, 2019). Naturally, this led to land-use changes, abandonment/expansion of cultivated lands, and a direct effect on industrial activities related to agriculture, such as the fertilizer industries.

One tracer of agricultural activity is atmospheric ammonia (NH_3), the main component of widely used nitrogen fertilizers that are essential for plant growth, such as urea and anhydrous NH_3 among other products (Finch et al., 2002). It is an alkaline, highly soluble and short-lived gas and the most abundant form of reactive nitrogen (Schlesinger and Hartley, 1992; Anderson et al., 2003). As the only alkaline gas in the atmosphere, it plays an important role in the acidity of cloud water, precipitation, and fine particulate matter ($PM_{2.5}$), as well as in the formation of the latter (Behera et al., 2013). Agriculture is the main anthropogenic contributor to the global NH_3 budget. Other sources are some types of industries (fertilizer, coking, soda ash, nickel, geothermal, and explosive), urban, biomass burning, and natural emissions such as seal colonies, seabirds and oceans (Theobald et al., 2006; Paulot et al., 2015; Whitburn et al., 2015; Riddick et al.,

[1] LATMOS/IPSL, Sorbonne Université, UVSQ, CNRS, Paris, France

[2] Université libre de Bruxelles (ULB), Spectroscopy, Quantum Chemistry and Atmospheric Remote Sensing (SQUARES), Brussels, Belgium

* Corresponding author:
Email: rimal.abeed@latmos.ipsl.fr

Downloaded from http://online.ucpress.edu/elementa/article-pdf/9/1/000041/483893/elementa.2021.000041.pdf by guest on 18 December 2021

2017; Van Damme et al., 2018; Chang et al., 2021). The excess in nitrogen in ecosystems leads to acidification of soil and water bodies and loss in biodiversity (Bobbink et al., 1998; Guthrie et al., 2018).

In this work, we investigate the war's effect on NH_3 concentrations in Syria. For this analysis, we rely on remote sensing data described in Section 2. In Section 3, we briefly discuss the main historical events that led to major land-use changes and fluctuations in NH_3 concentrations. In Section 4, we discuss the results of the case study of 1 fertilizer industry and agricultural region/land use change in the northeast part of Syria. In Section 5, we formulate our conclusions.

2. Materials and methods

2.1. Infrared atmospheric sounding interferometer (IASI) NH_3

IASI satellite instruments were launched onboard the polar-orbiting Metop platforms in October 2006 (IASI-A), September 2012 (IASI-B), and November 2018 (IASI-C). The instruments are nadir-looking Fourier-transform spectrometers that probe the Earth's atmosphere in the thermal infrared spectral range between 645 and 2,760 cm^{-1}, with a spectral resolution of 0.5 cm^{-1} (apodized). IASI monitors the atmospheric composition at any location 2 times per day, at around approximately 9:30 AM and PM (local time). Each instrument measures many of the chemical components that play a key role in the climate system and in several aspects of atmospheric pollution (Clerbaux et al., 2009).

The detection of NH_3 by IASI is done in the thermal infrared using its υ_2 vibrational band (approximately 950 cm^{-1}; Coheur et al., 2009). The NH_3 total columns exploited here were derived from IASI radiances using an Artificial Neural Network (Whitburn et al., 2016) and reanalyzed ERA-Interim data, ANNI-NH3-v2.1R (Van Damme et al., 2017). In the past, the IASI instrument has been used to identify, categorize, and quantify local hotspots of NH_3 (Van Damme et al., 2018). Numerous sources of NH_3 have been observed from IASI over the years (Clarisse et al., 2019a; Van Damme et al., 2021), being from agricultural practices and manure management, to industrial activities, in particular fertilizers industries (Van Damme et al., 2018; Dammers et al., 2019), fires (Coheur et al., 2009; Whitburn et al., 2015; Chang et al., 2021), and other natural sources (Clarisse et al., 2019b).

Only daytime measurements are considered in this study, as higher relative errors were observed from the nighttime measurements (Van Damme et al., 2017). The uncertainty estimates on the retrieved total columns can range from 5% to 1,000%; the lower uncertainties correspond to measurements during the day, in spring, and where NH_3 concentrations are high (Van Damme et al., 2017). In order to cover the period before and after the war in Syria with the same instrument, only IASI-A data are used. Comparison of NH_3 measurements from IASI with other satellite instruments, such as Crosstrack Infrared Sounder (Shephard and Cady-Pereira, 2015), exhibits consistent seasonal and interannual variability (Viatte et al., 2020). In a case study, Viatte et al. (2021) coupled ground-based measurement of NH_3 with IASI (on board Metop A, B, and C). The 2 instruments showed high agreement, with a Pearson's correlation coefficient $R = .75$. A recent validation of the IASI NH_3 product using reconstructed in situ columns based on aircraft profile measurements showed very good agreement (Guo et al., 2021).

In order to achieve a higher resolution spatial average, we averaged IASI-NH_3 total columns using an oversampling method, widely used in other studies for different trace gases concentrations using different instruments (Zhu et al., 2014; Van Damme et al., 2018).

2.2. Meteorology, land cover, and burned area

Relevant meteorological parameters used in this study are the skin temperature (T skin or land surface temperature), total precipitation, and near surface wind speed. The parameters are extracted daily from the European center for medium-range weather forecast's reanalysis (ERA5; Hersbach et al., 2020) and interpolated in time and space to the IASI morning observations. The resolution of ERA5 datasets is at $0.25 \times 0.25^\circ$ grid (native horizontal resolution of ERA5 is approximately 31 km). T skin is defined as the temperature of the surface at radiative equilibrium. It is derived from the surface energy balance within the land model in ERA5. The total precipitation product combines both large-scale and convective precipitations. The wind speed was calculated from the u and v wind components at 10 m of height above the surface of the Earth. The u component is defined as the horizontal wind speed heading toward the east, and the v component is the horizontal wind speed moving toward the north.

MODIS instruments are orbiting the Earth onboard the Aqua and Terra satellites. The Aqua/Terra MODIS Land Cover product (MCD12Q1 version 6) provides yearly maps of land cover with a 500 m spatial resolution for the period that extends from 2001 until 2019 (Sulla-Menashe and Friedl, 2018). The MOD12Q1 product employs 17 categories of land cover classification (Belward et al., 1999). In this work, we extract the croplands, shrub, and bare lands from these datasets to examine the effect of war and human displacement. The classification used in this study to represent croplands is defined as lands comprising of at least 60% cultivated area; A shrubland is defined as an area dominated by woody perennials (plants); Bare lands (also called *Barren* in the MCD12Q1 product) are defined as lands with an at least 60% non-vegetated area (Sulla-Menashe and Friedl, 2018). In an attempt to estimate the expansion/abandonment of croplands, we use the classes provided by the MODIS product. The yearly grid of 2011 is chosen as the base year; we compare the other years to it. This product agrees 73.6% with the Food and Agriculture Organization (FAO)-Land Cover Classification System (Sulla-Menashe et al., 2019). In addition to that, the percentage of pixels switching back and forth from a class to another (due to spectral similarity) was reduced from the previous version of the product to the current one (<30% for version 6 and 55% for version 5; Sulla-Menashe et al., 2019). Finally, we used the Aqua/Terra MODIS burned area product (MCD64A1) to look for fire events during the study period

Downloaded from http://online.ucpress.edu/elementa/article-pdf/9/1/000041/483893/elementa.2021.000041.pdf by guest on 18 December 2021

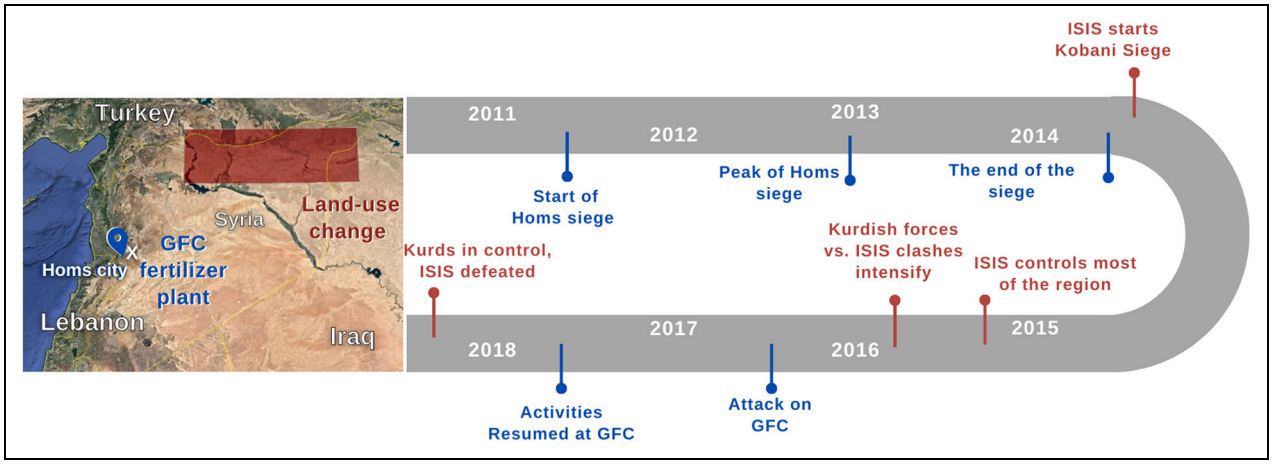


Figure 1. Graphical time line of the Syrian civil war events relevant to this study. In blue are those that affected the General Fertilizers Company (blue pin in left panel and discussed in Section 4.1), and in red are those associated to the land-use changes in the northeast region of interest (red box in left panel and discussed in Section 4.2). DOI: https://doi.org/10.1525/elementa.2021.000041.f1

(Giglio et al., 2018). This product provides the approximate date of burn and the extent of burned area with a 500-m resolution.

3. The conflict historical time line and evolution as related to this study

To understand the NH_3 variability for the 2 case studies discussed hereafter, we have listed the main relevant events and present them as a graphical time line in **Figure 1**. The General Fertilizers Company (GFC), a total of 3 plants, is first investigated in this study. Its location and remarkable events are shown in blue in **Figure 1**. It was affected by the siege of the city/region of Homs that started in May 2011 and peaked in 2013 when an external militia group intervened in the battle (ISW, 2013). The siege later ended in May 2014. Production in GFC between these dates was heavily affected. For example, during 2012, fertilizers production in GFC decreased dramatically due to the lack in fuel and electricity needs, as Islamic State in Iraq and Syria (ISIS) took over the nearby gas fields that were crucial for the production (Aita, 2020). Between 2014 and 2016, production was very low when compared to the prewar period, until an attack occurred on the plant itself during the second half of 2016 and the production stopped completely (FAO/WFP, 2017). The GFC plants resumed production in mid-July 2017 (Enab Baladi, 2019a; Aita, 2020).

On the other hand, in the northeastern part of the country (location and events shown in red in **Figure 1**), the most important series of events with direct effect on land use occurred a few years after the start of the war, in the period that extends from 2013 to 2019. ISIS started to infiltrate in the region during summer 2013 (Wilson Center, 2019). By January 2014, ISIS had already controlled a large part of the region shown in red in **Figure 1** (ISW, 2014). From September to December 2014, massive destruction was reported in regions close to the Turkish borders (included in our region of interest) due to the bombardments and clashes between ISIS and Kurdish forces (Walsh, 2014). ISIS continued to expand until it had seized a large area of the Syrian and the Iraqi territories in 2015. The croplands area increased during the occupation of ISIS. Later during 2015, the territory controlled by ISIS started to shrink according to studies conducted by IHS Markit (2017) as the Syrian Democratic Forces (commonly referred as Kurdish forces by media) started expelling ISIS from the area, until they eventually took control over most of northeast Syria by July 2019 (Liveumap, 2019). This occurred after confrontations that included Kurdish forces, Turkish military, and ISIS fighters as well as government and international troops. By 2017, ISIS had lost control of 98% of the territory claimed in 2015 (FOX 32, 2017; BBC, 2018). In 2019, freed from ISIS (BBC, 2019), the security conditions allowed a large increase in the croplands area.

4. Results and discussions

4.1. Temporal changes of NH_3 columns over a fertilizer factory

The GFC is located in Qattinah, south of Homs city (central Syria). The Homs city location is shown as a white cross in **Figure 1**. The company has been operating since 1972 and is owned by the Syrian government (Zammar et al., 2006). GFC is considered as one of the most important fertilizer production facilities in Syria, providing fertilizers for farmers all around the country. It was the only functioning fertilizers company in 2016 (FAO/WFP, 2017). GFC manufactures various fertilizer components and related products such as NH_3, urea, and nitric acid (Zammar et al., 2006). In October 2018, a Russian oil and gas company signed an investment contract with the Syrian government, which allows it to exploit the three main plants of GFC for 40 renewable years (Enab Baladi, 2019a; Al-Allaf and Said, 2021).

We used the IASI NH_3 daytime measurements to calculate total column daily averages around GFC. **Figure 2** illustrates the war effect on atmospheric NH_3. In panel

Downloaded from http://online.ucpress.edu/elementa/article-pdf/9/1/000041/483893/elementa.2021.000041.pdf by guest on 18 December 2021

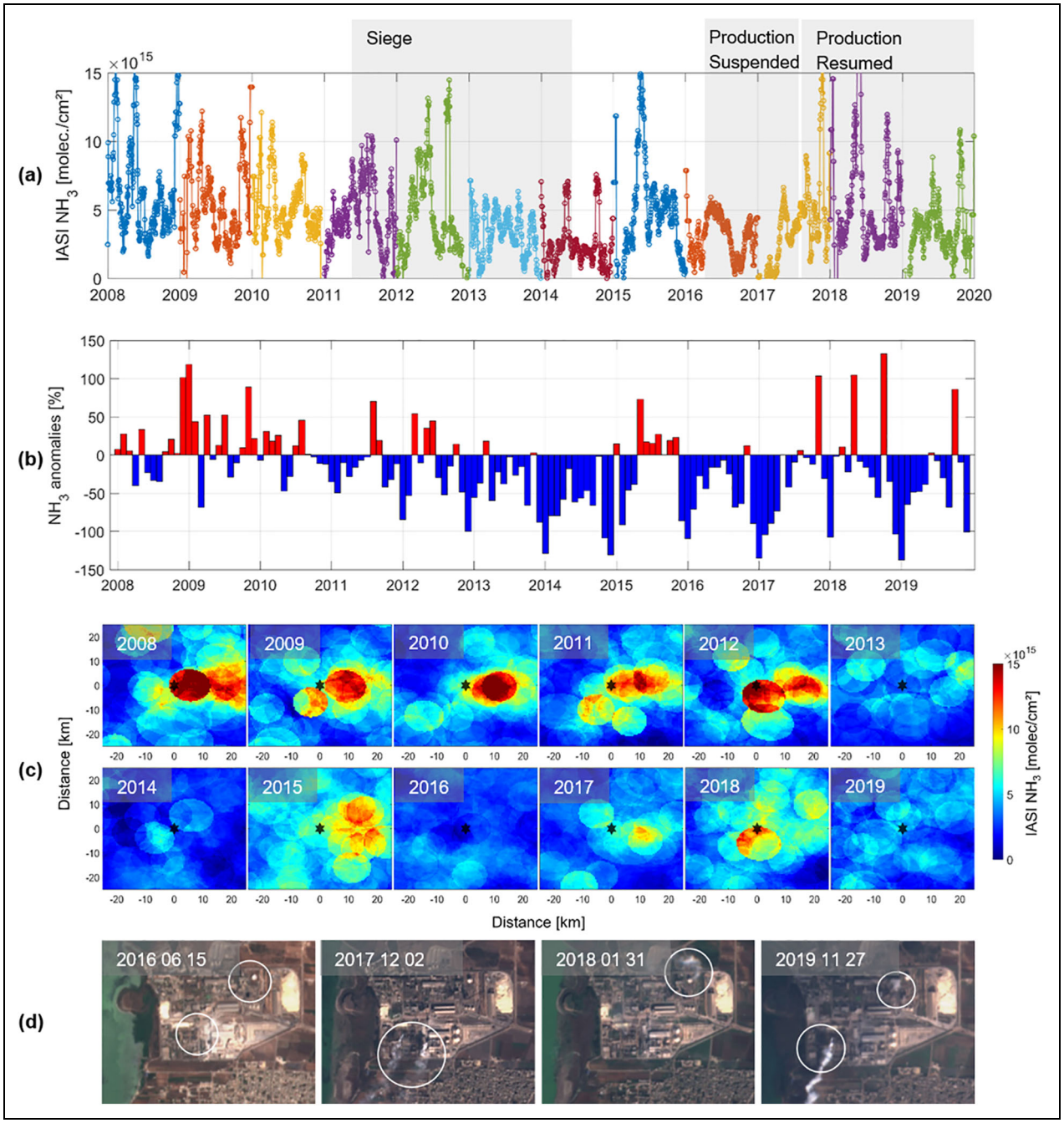


Figure 2. (a) 20-day running mean of IASI daily total columns of ammonia (molec/cm^2) averaged over the fertilizers industry (0.5 × 0.5° grid box centered on the factory). (b) Monthly percentage anomalies of IASI total columns of ammonia over the GFC, compared with [2008–2012] monthly averages. (c) Oversampled yearly spatial average of IASI NH_3 total columns (molec/cm^2) around the fertilizers industry (indicated with a black star). (d) Sentinel 2 L1C satellite images of the fertilizers company on days of suspension of activities (2016), and resume of production (2017, 2018 and end of 2019). DOI: https://doi.org/10.1525/elementa.2021.000041.f2

(a), we show the 20-day running mean of the NH_3 total columns. It corresponds to the average of a 0.5 × 0.5° grid box where the GFC is located in the center of the grid cell of data selection. Industries producing nitrogen-based fertilizers are known to be NH_3 sources, as NH_3 can be emitted through the synthesis of anhydrous NH_3, urea, and ammonium nitrate (EPA, 1995). A report from GFC mentioned that the off-gassing from the NH_3 production plant has a pungent odor, confirming the presence of NH_3 as well (Zammar et al., 2006). It can be seen that IASI NH_3 daily time series depends on the activity of the plant with clear perturbations that are related to the conflict events (shown in **Figure 1** and highlighted in **Figure 2**). We used the nonconflict years [2008–2012] as years with typical monthly variations, and we show the interannual variability before, during, and after the war (**Figure 2b**). Panel (b) in **Figure 2** shows monthly anomalies of NH_3 total columns with respect to the months in [2008–2012].

Downloaded from http://online.ucpress.edu/elementa/article-pdf/9/1/000041/483893/elementa.2021.000041.pdf by guest on 18 December 2021

Figure 2c shows the yearly spatial average using the oversampling method discussed in Section 2.1. Panels (a), (b), and (c) of **Figure 2** show a decrease in NH_3 total columns after 2012, in particular in 2013 and 2014, accounting to −17% and −47%, respectively, on a yearly average with respect to [2008–2012]. During these 2 years, the armed confrontations in the region included several military and militia groups, and the siege reached its peak by the end of 2013/early 2014.

The main factors that affected the GFC were the control of the gas field, that is essential for the production of the plant, by anti-government forces and ISIS (SANA, 2017; Aita, 2020); the attack on the company itself by anti-government groups during 2016 (as stated in **Figure 1**) which caused the activities to be suspended for a while (FAO/WFP, 2017); and finally, the shortage in employees (Enab Baladi, 2019a). From the monthly anomalies (**Figure 2b**), we can see that the interannual variations during 2013, 2014, and 2016 are larger than the typical variation observed before the intensification of the war events [2008–2012]. **Figure 2c** clearly shows a decrease in NH_3 columns over the fertilizer industry by −32% during 2016 in comparison to [2008–2012]. In mid-July 2017, after the Syrian military along with other militia groups took over Homs city in March (Washington Post, 2017), the GFC's NH_3 plant started functioning again (SANA, 2017; Enab Baladi, 2019a). To verify the timing of the suspension of activities, we also examined satellite visible images during the year 2016 from June and on, up till 2019. The result is shown in **Figure 2d**. We found that in 2016, the plant's chimney was not showing any visible exhaust plume, suggesting that it wasn't functioning after the attack took place. The figure also shows that in 2017 and 2018, the plant was functioning again with the chimney's typical exhaust (**Figure 2d**). The IASI measurement shows an increase in NH_3 in 2017 and 2018 in comparison to years without activity (2013, 2014, and 2016). During 2019, the production of the GFC was less than average (**Figure 2a–c**) due to shortage in fuel and electricity and because of the social conflicts in the company (Aita, 2020), with employees protesting against the new Russian investor company, and demanding better work conditions (COAR, 2019; The New Arab, 2019). It was also reported that productions were suspended for rehabilitation purposes during that year (FAO/WFP, 2019). By the end of 2019, the Russian company got in contact with many dismissed and retired employees offering them a job back at GFC with increased salaries and better conditions (Enab Baladi, 2019b). Satellite images at the end of 2019 revealed an increased activity of the industry (see **Figure 2d**); this observation agrees with the NH_3 concentration anomalies during that year (**Figure 2b**). Looking at a nearby NH_3 hot spot in the region, the soda ash industry in Turkey (Mersin: 36.789°N, 34.675°E), we find that while NH_3 concentrations decreased in 2016 for the GFC, the source in Mersin showed an increase and the NH_3 concentrations that became constantly higher than previous years (not shown here).

4.2. Land-use change in northeast Syria

Syria is divided into 14 governorates and the region of study, shown in a rectangle in **Figures 1** and **3**, comprises 4 governorates (a part of east Aleppo, half of Ar-Raqqa, most of Al-Hassakah, and a part of northern Deir Ez-Zor). This area was the most affected in comparison to other agricultural regions in Syria (FAO, 2017a; Mohamed et al., 2020). The climate is warm, semiarid with hot and dry summers (Faour et al., 2010; Al-Fares, 2013). From south to north, annual rainfall in the region ranges from 150 to 800 mm (Mohamed et al., 2020). The study region (39,889 km^2) comprises cultivated lands with livestock, mostly in the northern part close to the Turkish borders. Grains, cotton, fruits, and olives are cultivated, as well as nomadic herding and scattered cultivation take place in the southern part of the study area (Al-Fares, 2013). Syria's northeastern and southern parts are key regions for the agricultural sector; this is due to the favorable climate and the availability of water resources (Tull, 2017). We looked at MODIS land cover type for the period [2008–2019].

Figure 3a shows 4 snapshots of the land cover in northeast Syria for 4 key years that correspond to beginning of the war (2011), maximum control of ISIS (2015), intense clashes between ISIS and Kurdish forces (2017), and improved security conditions (2019). More information on detailed events are listed in Section 3. **Figure 3b** shows 3 snapshots of the change in MODIS croplands for 2015, 2017, and 2019 as compared to 2011. Croplands expansion is represented in red (cultivated croplands) and abandonment of croplands is shown in blue (neglected croplands). We chose 2011 as a reference year since the Syrian civil war began in March of that year. The area cultivated in 2011 did not change drastically from previous years. Despite the fact that we do not see major changes in croplands' area during 2011, farmers were struggling to travel long distances due to security reasons which prevented them from migrating to the southern part of Syria for agricultural labor (FAO, 2012), a pattern reported in previous years (Selby et al., 2017). As a result, the livestock sector has been affected as herders rely on migration to areas with abundant grasslands and water for their herds. We note also that the study region was still under the control of the Syrian government and that the armed oppositions only started later during 2012 (ISW, 2012). Up until 2015, we observed an increase in cultivated area from 2011 by 7%, 9%, and 10.5% in 2013, 2014, and 2015, respectively (only 2015 is shown here). The increase is especially widespread in Al-Hassakah governorate on the east of the study region (location is shown in **Figure 3b**). In fact, by December 2014, farmers in areas controlled by ISIS found themselves obligated to cultivate their lands, as ISIS issued a law stating that it will confiscate any abandoned cropland (Al-Tamimi, 2015). By mid-2015, ISIS started losing its control gradually. This can particularly be seen in 2017's land-use change shown in **Figure 3b** where we observe a decrease in croplands area (by −14% as compared to 2011) and an increase in bare lands as well as shrublands. The clashes intensified when the Kurdish forces pushed ISIS fighters out of the region. FAO report states that in 2017, the fighting and airstrikes

Downloaded from http://online.ucpress.edu/elementa/article-pdf/9/1/000041/483893/elementa.2021.000041.pdf by guest on 18 December 2021

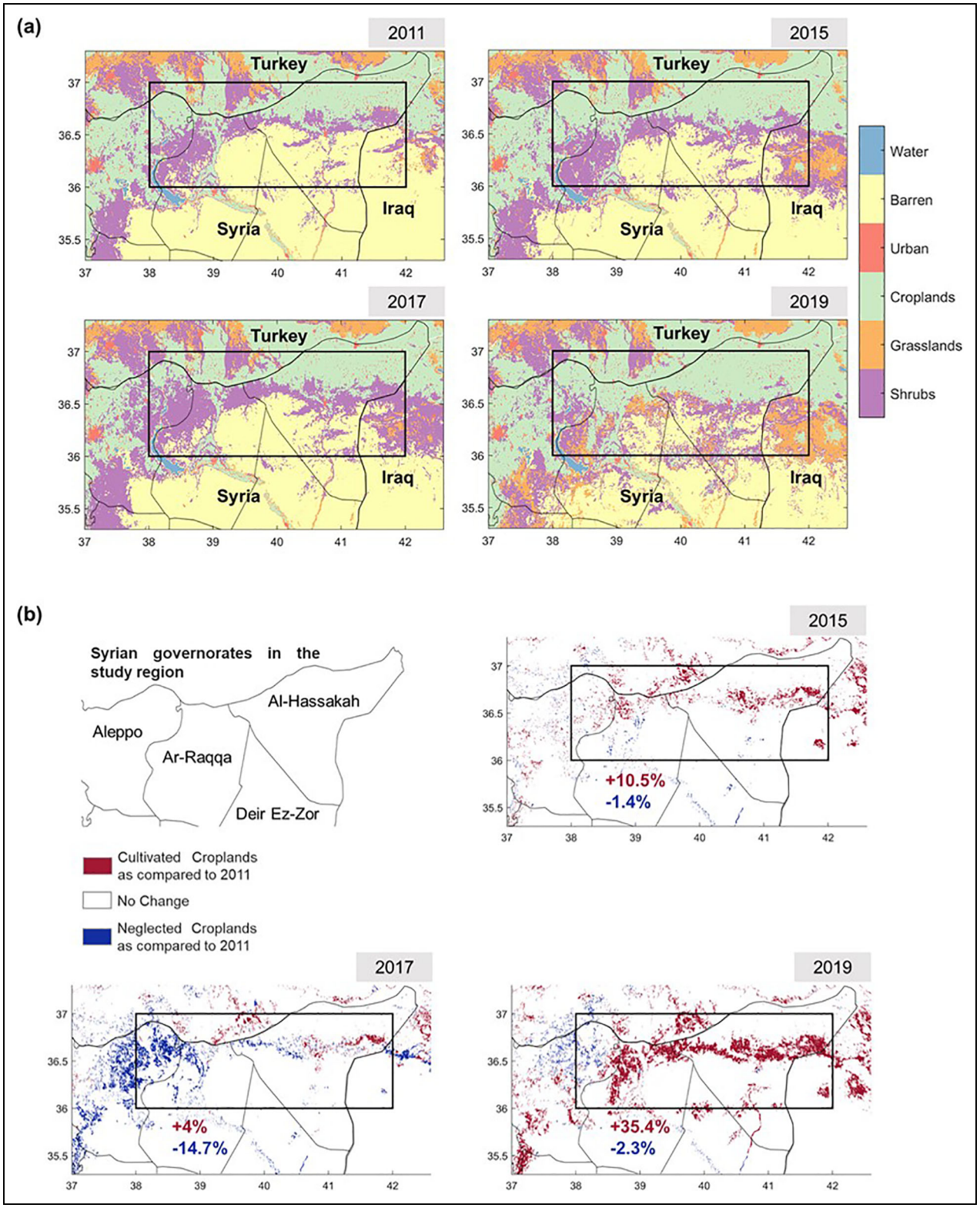


Figure 3. (a) Yearly distribution of MODIS land cover over northeast Syria (500 × 500 m^2). The region of study is shown in the black rectangle for the years 2011 (start of the war), 2015 (Islamic State in control of most of the region), 2017 (intense clashes between Islamic State, Kurdish forces and other groups), and 2019 (better security conditions). Only relevant land cover classifications are shown here; (b) Yearly evolution (neglected or cultivated) of MODIS croplands as compared to croplands for the year 2011. "Cultivated Croplands" (red pixels)/"Neglected Croplands" (blue pixels) represent croplands that were cultivated/abandoned during the designated year in comparison to 2011. The evolution (expansion/abandonment) of croplands (indicated in red/blue) is calculated in comparison to 2011 and for pixels located in Syria only. DOI: https://doi.org/10.1525/elementa.2021.000041.f3

Downloaded from http://online.ucpress.edu/elementa/article-pdf/9/1/000041/483893/elementa.2021.000041.pdf by guest on 18 December 2021

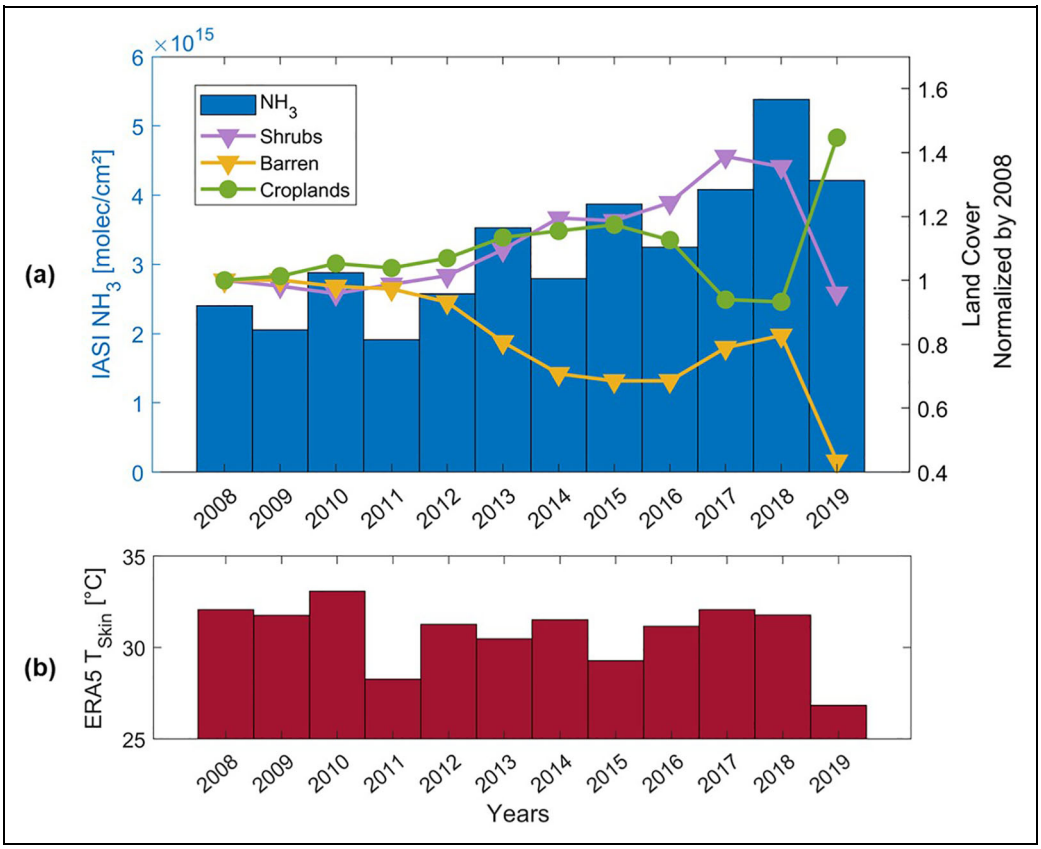


Figure 4. (a) Spring IASI NH_3 total columns [March–April–May] over the region of study (in blue), yearly MODIS Land Cover Types normalized by 2008: Shrublands (in purple), bare lands (in yellow), and croplands (in green) for the same region; (b) ERA5 T skin averaged during the spring season of each year. DOI: https://doi.org/10.1525/elementa.2021.000041.f4

resumed in Ar-Raqqa, which constrained the humanitarian access to civilians (FAO, 2017b). Despite the improvement in security in some parts of the country, the situation in northeast Syria led to displacement of the civilians, and this can explain the abandoned farmlands seen in 2017 in **Figure 3** (FAO, 2017c). In fact, the 4 governorates included in our region of study were classified as regions where agricultural loss exceeds US$1.5 billion which was considered the highest amount of financial damage in the country (FAO, 2017a).

During 2019, an increase in the cultivated area of approximately +35% compared to 2011 can be seen over the whole Syrian area of study (**Figure 3b**). The change represents shrublands and bare lands that had shifted into croplands (cropland expansion). The improvement in security conditions and the favorable rainfall during 2018/2019 winter season caused an expansion in the area cultivated with cereals (FAO, 2019). During that year, the area cultivated in Al-Hassakah, Aleppo, and Ar-Raqqa represented 70% of the total cultivated wheat area in the whole country (FAO, 2020). Kurdish forces had controlled almost all of the territory of northeast Syria by July 2019 (Liveumap, 2019), and normal living and farming conditions are restored since.

In **Figure 4a**, we show the NH_3 evolution in the study region during the spring season (MAM) and over the whole period [2008–2019]. Croplands (in green), shrublands (in purple), and bare lands (in yellow) changes per year are also added. To assess the effect of soil temperature on NH_3 concentrations, we also show the T skin evolution in **Figure 4b** over the same area from ERA5. It has been shown in previous studies that the rate of emission of NH_3 from the soil upon the application of fertilizers is mostly affected by temperature and humidity of the soil and air among other factors (Sharpe and Harper, 1995; Anderson et al., 2003; Le Cadre et al., 2005; Dari et al., 2019).

We choose the spring season because we are interested in the NH_3 change related to agricultural activities and fertilizer use. Generally, 2 NH_3 column peaks are observed per year in the study region; the first and the highest is in spring (between March and mid-May); the second is in autumn and is lower (and not discussed here). Over the period that extends from 2008 to 2019, NH_3 columns show a general increase in concentrations above the study region. We can see that NH_3 fluctuations over the years before the war (2011) are dependent on both land cover changes and T skin (**Figure 4b**). For example, and in particular during the [2008–2012] period, the NH_3 interannual variability was mostly governed by temperature fluctuations, as the land cover was mostly constant. However, during the occupation of ISIS [2013–2015], cultivated area increased, and as such, it was an important driver in the NH_3 variability: the percentage increase in

Downloaded from http://online.ucpress.edu/elementa/article-pdf/9/1/000041/483893/elementa.2021.000041.pdf by guest on 18 December 2021

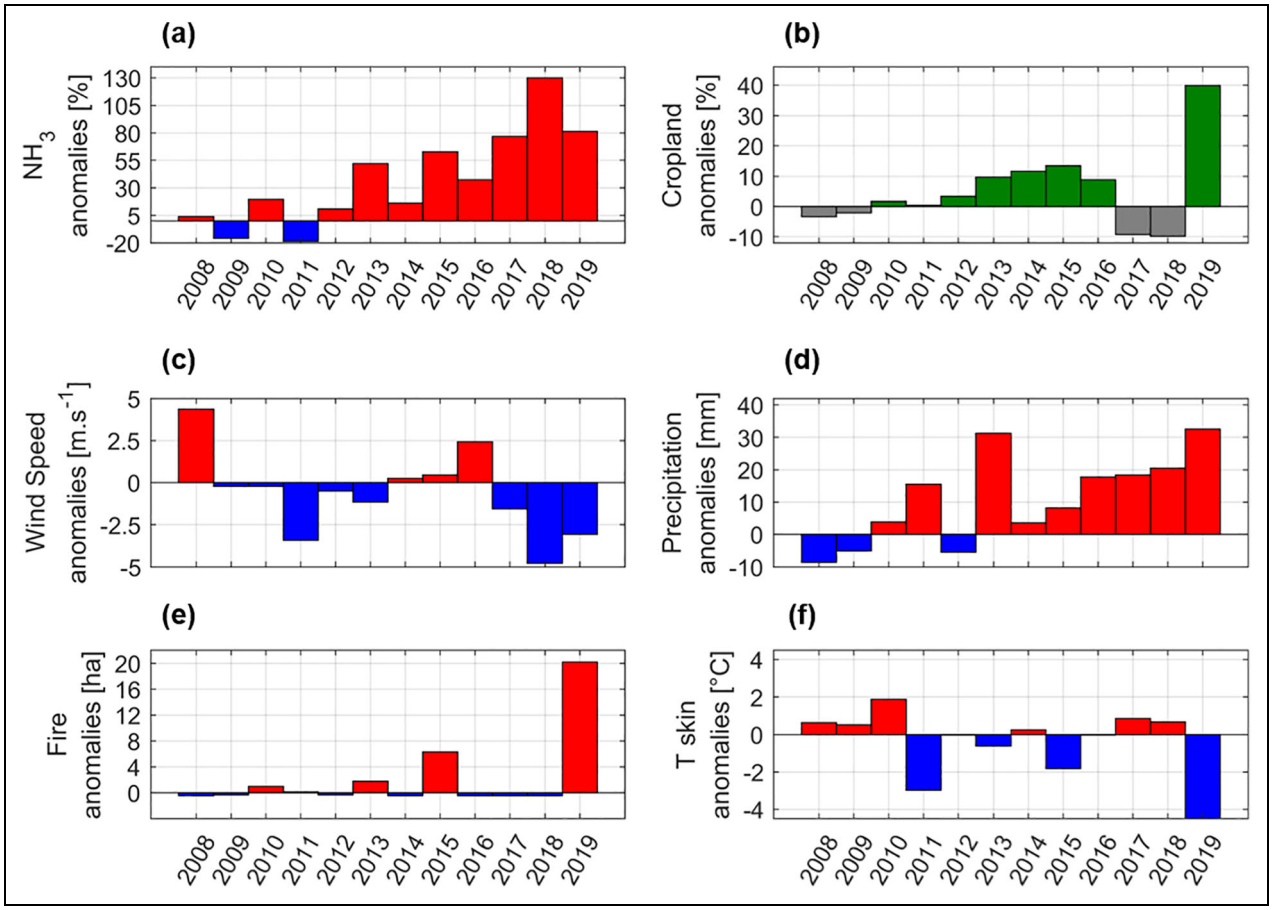


Figure 5. Spring anomalies over the region of study compared to the average of the spring season of [2008–2012] for (a) IASI NH_3 total columns [%], (b) cropland anomalies [%], (c) ERA5 wind speed anomalies [m/s], (d) ERA5 total precipitation anomalies [mm], (e) MODIS burned area [ha], and (f) ERA5 T skin anomalies [°C]. DOI: https://doi.org/10.1525/elementa.2021.000041.f5

NH_3 concentrations during [2013–2015] is estimated to be +44% in comparison to the average of [2008–2012]. As discussed earlier, the Kurdish forces were pushing ISIS out of the region by mid-2015. We observe an increase in croplands area, and the NH_3 keeps increasing after 2015. Simultaneously, both shrublands and bare lands are observed to be inversely correlated to croplands area. The figure shows that the croplands' expansion/cultivation reaches a maximum in 2019. The difference in NH_3 concentration during the period [2016–2019] in comparison to [2008–2012] average was found to be +81%, while T skin slightly decreased (–0.25%). Finally, croplands, over the same period, showed a decrease in 2017 (–14%) and 2018 (–15%), and an increase in 2019 (+35%) compared to 2011.

In order to check the effect of the different meteorological variables on NH_3 concentrations, we show in **Figure 5** the anomalies of NH_3 in panel (a) in the study region during the spring season (MAM) relative to the average of spring (2008–2012). Panel (b) shows the yearly cropland anomalies with respect to [2008–2012]. Panels (c) and (d) show the spring anomalies of ERA5 wind speed and total precipitation respectively for the same region and relative to the spring average of [2008–2012]. Panel (e) shows MODIS burned area during the spring season, and panel (f) shows ERA5T skin anomalies for the same season and time period, as compared to the spring average of [2008–2012].

During normal conditions prior to the war (2008–2012), NH_3 anomalies fluctuated between ±20% (**Figure 5a**), temperature anomalies varied between –3°C and +2°C (**Figure 5f**), while croplands anomalies fluctuated between ±3.3% (**Figure 5b**). During the occupation of ISIS that started in 2013 and reached a maximum of land-control by 2015, anomalies in NH_3 concentrations kept increasing (+52%, +16%, and +63% for the years 2013, 2014, and 2015, respectively). The T skin anomalies during these years were relatively normal (see **Figure 5f**). The corresponding T skin anomalies for 2013, 2014, and 2015, respectively, are –0.62°C, +0.24°C, and –1.82°C (–2%, +0.8%, and –6%). While the production of fertilizers in Syria (and in GFC) decreased dramatically during the war, the imported quantity of nitrate-based fertilizers (NPK) increased from 2,634 tons in 2013 to 12,356 tons in 2019 (FAOSTAT, 2021); this explains the continuous availability of nitrogen-based fertilizers in the market.

Precipitation anomalies (**Figure 5d**) for the whole period fluctuated between –10 and +20 mm/season except during 2013 and 2019 (+31 and +32 mm/season respectively). We notice that the croplands' area in 2019 is

Downloaded from http://online.ucpress.edu/elementa/article-pdf/9/1/000041/483893/elementa.2021.000041.pdf by guest on 18 December 2021

higher than that in 2018, but NH_3 concentrations are lower in 2019. The higher precipitation anomalies (+32 mm/season) in 2019 and the lower T skin anomalies (–4.5°C) are most likely the reason of the reduction in NH_3 concentrations despite the cropland expanding during that year (due to the solubility of NH_3 in aqueous phases, precipitation causes the wet deposition of NH_3 on surfaces). Fires do not occur frequently during the spring season in that region; however, we can see that MODIS burned area product shows +6.3 and +20.2 ha of burned area in 2015 and 2019, respectively (**Figure 5e**); these fires may have contributed to the concentrations of NH_3. In the period before the war (2008–2012), the wind speed anomalies fluctuated between –3.4 and +4.4 m/s (**Figure 5c**); however, in 2018, wind speed decreased by –4.8 m/s, that is, outside the usual fluctuation during [2008–2012]. As observed, NH_3 is highest in 2018 (**Figure 5a**). Fires did not occur during the spring season of 2018, and precipitations were within the usual fluctuation range of [2008–2012]. In fact, the lower wind speed observed in 2018 might have led to the persistence of NH_3. To conclude, wind speed, fire events, and precipitation were shown to be within the normal range, except perhaps for 2018 (lower wind speed, higher NH_3) and 2019 (more precipitation, more fire events, but lower skin temperature). As such, the other years are most likely affected by the croplands' expansion. As such, fertilizer use is most likely the main driver for the increase in NH_3 concentrations.

5. Discussion and conclusions

In this study, we discuss the effects of war in breaking the usual NH_3 interannual variation in the atmosphere. IASI observations show that NH_3 variability is driven by both natural factors and political events, such as in the case of the Syrian civil war. While the conflict is responsible for the reduced NH_3 concentrations around the GFC industrial plant due to reduced emissions, it was also responsible for an actual increase of NH_3 in the northeast due to the expansion of agricultural lands. Our work shows that remote sensing data acquired from space can help the monitoring of socio-ecological changes caused by wars and political conflicts down to a local scale.

We described case studies of 2 NH_3 source regions in Syria and their disruptions due to the conflict. The first is over a fertilizer industry in the city of Homs where industrial activities have been disrupted by the war, and the second over an agricultural region in northeast Syria. A decrease in NH_3 concentration is observed over the fertilizers industry due to the siege and its consequences reading –17%, –47%, and –32% in 2013, 2014, and 2016, respectively, as compared to the [2008–2012] average. Even after the fertilizer industry started functioning again in 2017, the seasonal variation and concentration of NH_3 were never the same as the period that preceded the beginning of the civil war. The activity of the fertilizers industry was affected by shortage in workforce, battles, and politics.

In northeast Syria, the fluctuation in IASI NH_3 columns is seen to be affected by T skin before the war (2011) and most likely driven by changes in land cover after 2011. The area witnessed abandonment of croplands in 2017 (–14%), in comparison to 2011, but also a huge croplands expansion in 2019 (+35%). The presence of ISIS in northeast Syria has changed cropping patterns and forced farm owners to cultivate their lands (Jaafar and Woertz, 2016).

We observed clear disruptions in both regions examined in this study. Although the availability of fertilizers in the market would have been affected by the halt of the GFC, the gap in the market was met with imported fertilizers (both legally and illegally). In addition to that, both regions were witnessing different events in different timeframes, which makes it hard to draw a connection between the 2 case studies.

This study combines local IASI NH_3 observations with ERA5 meteorological products (temperatures, total precipitation, and wind speed) and MODIS land cover and burned area. It could be extended to other parts of the world in order to analyze how political changes influence agricultural practices and industrial activities (e.g., in Afghanistan before and after 2021). Current emission inventories do not consider war-related events; we think that they should be adapted according to the results of this study and other studies that show disruptions in emissions that are not related only to climatology. The long-term homogeneous IASI dataset, whose continuity will be ensured with the IASI-NG mission (Crevoisier et al., 2014) that should fly from 2023 to 2050, offer a unique tool to monitor the impact of societal changes and perturbations on the atmospheric composition.

Data accessibility statement

The IASI-NH_3 used in this study are retrieved from the Aeris data infrastructure (https://iasi.aeris-data.fr/nh3r-era5/). MODIS land cover data are available for download in the following link: https://doi.org/10.5067/MODIS/MCD12Q1.006. MODIS fire data are available for download in the following link: https://lpdaac.usgs.gov/products/mcd64a1v061/. Images from Sentinel 2 L1C are available at https://apps.sentinel-hub.com/sentinel-playground. ERA5 skin temperature, 10 m u and v wind components, and total precipitation from 1979 to present are available for download in the following DOI: 10.24381/cds.adbb2d47.

Acknowledgments

The authors acknowledge the Aeris data infrastructure for providing the IASI L1C and L2 data. Rimal Abeed is grateful to CNES for financial support. The IASI mission is a joint mission of Eumetsat and the Centre National d'Etudes Spatiales (CNES, France).

Funding

The research was funded by the F.R.S.-FNRS and the Belgian State Federal Office for Scientific, Technical and Cultural Affairs (Prodex arrangement HIRS). M. Van Damme is Postdoctoral Researcher (Chargé de Recherche) and L. Clarisse is Research Associate (Chercheur Qualifié) both supported by the Belgian F.R.S.-FNRS.

Downloaded from http://online.ucpress.edu/elementa/article-pdf/9/1/000041/483893/elementa.2021.000041.pdf by guest on 18 December 2021

Competing interests

The authors are aware of no competing interests.

Author contributions

Contributed to conception and design: RA, SS.

Contributed to acquisition of data: MVD, LC.

Contributed to analysis and interpretation of data: RA.

Drafted and/or revised the article: RA, SS, CC, MVD, LC, PFC.

Approved the submitted version for publication: RA, SS, CC, MVD, LC, PFC.

References

Aita, S. 2020, Dec. *The unintended consequences of U.S. and European unilateral measures on Syria's economy and its small and medium enterprises.* Atlanta, GA: The Carter Center. Available at https://www.cartercenter.org/resources/pdfs/peace/conflict_resolution/syria-conflict/syria-unintended-consequences-aita-12-20.pdf.

Al-Allaf, A, Said, S. 2021. Russian investment in Syrian phosphate: Opportunities and challenges. *Publications Office of the European Union*. (2021/04). DOI: http://dx.doi.org/10.2870/42382.

Al-Fares, W. 2013. Historical land use/land cover classification using remote sensing: A case study of the Euphrates river basin in Syria. Heidelberg, Germany. *SpringerBriefs in Geography*. DOI: http://dx.doi.org/10.1007/978-3-319-00624-6.

Al-Tamimi, AJ. 2015. Archive of Islamic State administrative documents. Available at http://www.aymennjawad.org/2015/01/archive-of-islamic-state-administrative-documents. Accessed 13 April 2021.

Anderson, N, Strader, R, Davidson, C. 2003. Airborne reduced nitrogen: Ammonia emissions from agriculture and other sources. *Environment International* **29**(2–3): 277–286. DOI: http://dx.doi.org/10.1016/S0160-4120(02)00186-1.

BBC. 2018, 28 Mar. Islamic State and the crisis in Iraq and Syria in maps. *BBC News*. Available at https://www.bbc.com/news/world-middle-east-27838034. Accessed 26 March 2021.

BBC. 2019, 23 Mar. Islamic State group defeated as final territory lost, US-backed forces say. *BBC News*. Available at https://www.bbc.com/news/world-middle-east-47678157. Accessed 26 March 2021.

Behera, SN, Betha, R, Liu, P, Balasubramanian, R. 2013. A study of diurnal variations of $PM_{2.5}$ acidity and related chemical species using a new thermodynamic equilibrium model. *Science of the Total Environment* **452–453**: 286–295. DOI: http://dx.doi.org/10.1016/j.scitotenv.2013.02.062.

Belward, AS, Estes, JE, Kline, KD. 1999. The IGBP-DIS global 1-km land-cover data set DIS-Cover: A project overview. *Photogrammetric Engineering & Remote Sensing* **65**(9): 1013–1020.

Bobbink, R, Hornung, M, Roelofs, JGM. 1998. The effects of air-borne nitrogen pollutants on species diversity in natural and semi-natural European vegetation. *Journal of Ecology* **86**(5): 717–738. DOI: http://dx.doi.org/10.1046/j.1365-2745.1998.8650717.x.

Chang, Y, Zhang, YL, Kawichai, S, Wang, Q, Van Damme, M, Clarisse, L, Prapamontol, T, Lehmann, MF. 2021. Convergent evidence for the pervasive but limited contribution of biomass burning to atmospheric ammonia in peninsular Southeast Asia. *Atmospheric Chemistry and Physics* **21**(9): 7187–7198. DOI: http://dx.doi.org/10.5194/acp-21-7187-2021.

Clarisse, L, Van Damme, M, Clerbaux, C, Coheur, PF. 2019a. Tracking down global NH_3 point sources with wind-adjusted superresolution. *Atmospheric Measurement Techniques* **12**(10): 5457–5473. DOI: http://dx.doi.org/10.5194/amt-12-5457-2019.

Clarisse, L, Van Damme, M, Gardner, W, Coheur, PF, Clerbaux, C, Whitburn, S, Hadji-Lazaro, J, Hurtmans, D. 2019b. Atmospheric ammonia (NH_3) emanations from Lake Natrons saline mudflats. *Scientific Reports* **9**(1): 4441. DOI: http://dx.doi.org/10.1038/s41598-019-39935-3.

Clerbaux, C, Boynard, A, Clarisse, L, George, M, Hadji-Lazaro, J, Herbin, H, Hurtmans, D, Pommier, M, Razavi, A, Turquety, S, Wespes, C, Coheur, PF. 2009. Monitoring of atmospheric composition using the thermal infrared IASI/MetOp sounder. *Atmospheric Chemistry and Physics* **9**(16): 6041–6054. DOI: http://dx.doi.org/10.5194/acp-9-6041-2009.

COAR. 2019. *Syria update: April 04–April 10, 2019*. Center for Operational Analysis and Research. Available at https://coar-global.org/2019/04/10/syria-update-between-04-april-to-10-april-2019/.

Coheur, PF, Clarisse, L, Turquety, S, Hurtmans, D, Clerbaux, C. 2009. IASI measurements of reactive trace species in biomass burning plumes. *Atmospheric Chemistry and Physics* **9**(15): 5655–5667. DOI: http://dx.doi.org/10.5194/acp-9-5655-2009.

Corbane, C, Kemper, T, Freire, S, Louvrier, C, Pesaresi, M. 2016. *Monitoring the Syrian humanitarian crisis with the JRCs global human settlement layer and night-time satellite*. Publications Office of the European Union (EUR 27933). DOI: http://dx.doi.org/10.2788/48956.

Crevoisier, C, Clerbaux, C, Guidard, V, Phulpin, T, Armante, R, Barret, B, Camy-Peyret, C, Chaboureau, JP, Coheur, PF, Crépeau, L, Dufour, G, Labonnote, L, Lavanant, L, Hadji-Lazaro, J, Herbin, H, Jacquinet-Husson, N, Payan, S, Péquignot, E, Pierangelo, C, Sellitto, P, Stubenrauch, C. 2014. Towards IASI-New Generation (IASI-NG): Impact of improved spectral resolution and radiometric noise on the retrieval of thermodynamic, chemistry and climate variables. *Atmospheric Measurement Techniques* **7**(12): 4367–4385. DOI: http://dx.doi.org/10.5194/amt-7-4367-2014.

Dammers, E, McLinden, CA, Griffin, D, Shephard, MW, Van Der Graaf, S, Lutsch, E, Schaap, M, Gainairu-Matz, Y, Fioletov, V, Van Damme, M,

Downloaded from http://online.ucpress.edu/elementa/article-pdf/9/1/000041/483893/elementa.2021.000041.pdf by guest on 18 December 2021

Whitburn, S, Clarisse, L, Cady-Pereira, K, Clerbaux, C, Coheur, PF, Erisman, JW. 2019. NH_3 emissions from large point sources derived from CrIS and IASI satellite observations. *Atmospheric Chemistry and Physics* **19**(19): 12261–12293. DOI: http://dx.doi.org/10.5194/acp-19-12261-2019.

Dari, B, Rogers, CW, Walsh, OS. 2019. *Understanding factors controlling ammonia volatilization from fertilizer nitrogen applications* (Extension Bulletin 927). University of Idaho. Available at https://www.extension.uidaho.edu/publishing/pdf/BUL/BUL926.pdf.

Eklund, L, Degerald, M, Brandt, M, Prishchepov, AV, Pilesjö, P. 2017. How conflict affects land use: Agricultural activity in areas seized by the Islamic State. *Environmental Research Letters* **12**(5): 054004. DOI: http://dx.doi.org/10.1088/1748-9326/aa673a.

Enab Baladi. 2019a, 31 Jan. *General Fertilizers Company: From Syrian stumbling and Iranian competition to Russian takeover*. Enab Baladi. Available at https://english.enabbaladi.net/archives/2019/01/general-fertilizers-company-from-syrian-stumbling-and-iranian-competition-to-russian-takeover/. Accessed 18 March 2021.

Enab Baladi. 2019b, 12 Sep. *Russia to return dismissed employees to fertilizers company in Homs*. Enab Baladi. Available at https://english.enabbaladi.net/archives/2019/09/russia-to-return-dismissed-employees-to-fertilizers-company-in-homs/. Accessed 23 March 2021.

EPA. 1995. Inorganic chemical industry, in *Stationary point and area sources: AP-42, compilation of air pollutant emissions factors*, Vol. 1, 5th ed. U.S. Environmental Protection Agency. Available at https://www.epa.gov/air-emissions-factors-and-quantification/ap-42-fifth-edition-volume-i-chapter-8-inorganic-chemical-0. Accessed 09 April 2021.

FAO. 2012. GIEWS country briefs: Syrian Arab Republic. Rome. Available at https://reliefweb.int/report/syrian-arab-republic/giews-country-briefs-syrian-arab-republic-14-march-2012.

FAO. 2017a. Counting the cost: Agriculture in Syria after six years of crisis. Rome. Available at http://www.fao.org/fileadmin/user_upload/emergencies/docs/FAO_SYRIA-counting-the-cost.pdf.

FAO. 2017b. Syrian Arab Republic situation report. Rome. Available at http://www.fao.org/fileadmin/user_upload/emergencies/docs/FAOSyria_SitReport-JULY2017.pdf.

FAO. 2017c. Syrian Arab Republic situation report. Rome. Available at http://www.fao.org/fileadmin/user_upload/emergencies/docs/FAOSyriaSitRep_Nov2017.pdf.

FAO. 2019. GIEWS country briefs: Syrian Arab Republic. Rome. Available at https://reliefweb.int/report/syrian-arab-republic/giews-country-brief-syrian-arab-republic-reference-date-05-september.

FAO. 2020. 2019 – 2020 Agriculture seasonal performance—key updates. Available at https://fscluster.org/sites/default/files/documents/fao_presentation-seasonal_update_july_2020.pdf. Accessed 13 April 2021.

FAO/WFP, 2017. Special report: Crop and food security assessment mission to the Syrian Arab Republic. Rome. Available at http://www.fao.org/3/i7578e/i7578e.pdf.

FAO/WFP. 2019. Special report: Crop and food security assessment mission to the Syrian Arab Republic. Rome. Available at https://reliefweb.int/report/syrian-arab-republic/special-report-faowfp-crop-and-food-security-assessment-mission-syrian-3.

FAOSTAT. 2021. *FAOSTAT: Fertilizers by Product*. Available at https://knoema.com/FAORFBFP/faostat-fertilizers-by-product. Accessed 8 Aug 2021.

Faour, G, Meslmani, Y, Fayad, A. 2010. Climate-change atlas of Syria. DOI: http://dx.doi.org/10.13140/RG.2.2.26562.17601.

Finch, HJS, Samuel, AM, Lane, GPF. 2002. Fertilisers and manures, in *Lockhart and Wisemans Crop Husbandry Including Grassland*. 8th ed. Cambridge: 52–78 (Woodhead Publishing Series in Food Science, Technology and Nutrition). DOI: http://dx.doi.org/10.1533/9781855736504.1.52. Accessed 04 March 2021.

FOX 32. 2017. ISIS has lost 98 percent of its territory, officials say. *FOX 32 Chicago*. Available at https://www.fox32chicago.com/news/isis-has-lost-98-percent-of-its-territory-officials-say. Accessed 26 March 2021.

Giglio, L, Boschetti, L, Roy, D P, Humber, ML, Justice, CO. 2018. The collection 6 MODIS burned area mapping algorithm and product. *Remote Sensing of Environment* **217**: 72–85. DOI: http://dx.doi.org/10.1016/j.rse.2018.08.005.

Guo, X, Wang, R, Pan, D, Zondlo, MA, Clarisse, L, Van Damme, M, Whitburn, S, Coheur, PF, Clerbaux, C, Franco, B, Golston, LM, Wendt, L, Sun, K, Tao, L, Miller, D, Mikoviny, T, Müller, M, Wisthaler, A, Tevlin, AG, Murphy, JG, Nowak, JB, Roscioli, JR, Volkamer, R, Kille, N, Neuman, JA, Eilerman, SJ, Crawford, JH, Yacovitch, TI, Barrick, JD, Scarino, AJ. 2021. Validation of IASI satellite ammonia observations at the pixel scale using in situ vertical profiles. *Journal of Geophysical Research: Atmospheres* **126**(9). DOI: http://dx.doi.org/10.1029/2020JD033475.

Guthrie, S, Dunkerley, F, Tabaqchali, H, Harshfield, A, Ioppolo, B, Manville, C. 2018. *Impact of ammonia emissions from agriculture on biodiversity: An evidence synthesis. RAND Corporation*. The Royal Society (RR-2695-RS). DOI: http://dx.doi.org/10.7249/RR2695.

Hersbach, H, Bell, B, Berrisford, P, Hirahara, S, Horányi, A, Muñoz-Sabater, J, Nicolas, J, Peubey, C, Radu, R, Schepers, D, Simmons, A, Soci, C, Abdalla, S, Abellan, X, Balsamo, G, Bechtold, P, Gionata Biavati, G, Bidlot, J, Bonavita, M, De Chiara, G, Dahlgren, P, Dee, D, Diamantakis, M, Dragani, R, Flemming, J, Forbes, R, Manuel Fuentes, M, Geer, A, Haimberger, L, Healy, S,

Downloaded from http://online.ucpress.edu/elementa/article-pdf/9/1/000041/483893/elementa.2021.000041.pdf by guest on 18 December 2021

Hogan, RJ, Elías Hólm, E, Janisková, M, Keeley, S, Laloyaux, P, Lopez, P, Lupu, C, Radnoti, G, de Rosnay, P, Rozum, I, Vamborg, F, Villaume, S, Thépaut, JN. 2020. The ERA5 global reanalysis. *Quarterly Journal of the Royal Meteorological Society* **146**(730): 1999–2049. DOI: http://dx.doi.org/10.1002/qj.3803.

IHS Markit. 2017, 10 Oct. *Islamic State in decline*. IHS Markit. Available at https://ihsmarkit.com/research-analysis/islamic-state-in-decline.html.

ISW. 2012. *Syrias maturing insurgency*. Institute for the Study of War. Available at http://www.understandingwar.org/sites/default/files/Syrias_MaturingInsurgency_21June2012.pdf.

ISW. 2013. *Syria update: The fall of al-Qusayr*. Institute for the Study of War. Available at http://www.understandingwar.org/backgrounder/syria-update-fall-al-qusayr.

ISW. 2014. *Middle East Security Report 22*. Institute for the Study of War. Available at http://www.understandingwar.org/sites/default/files/ISIS_Governance.pdf.

Jaafar, HH, Woertz, E. 2016. Agriculture as a funding source of ISIS: A GIS and remote sensing analysis. *Food Policy* **64**: 14–25. DOI: http://dx.doi.org/10.1016/j.foodpol.2016.09.002.

Le Cadre, E, Genermont, S, Decuq, C, Recous, S, Cellier, P. 2005. A laboratory system to estimate ammonia volatilization. *Agronomy for Sustainable Development* **25**(1): 101–107. DOI: http://dx.doi.org/10.1051/agro:2004060.

Liveumap. 2019, 31 Aug. *Day of news on live map* (Live Universal Awareness Map). Virgina. Available at https://syria.liveuamap.com/en/time/31.08.2019. Accessed 26 March 2021.

Mohamed, M, Anders, J, Schneider, C. 2020. Monitoring of changes in Land Use/Land Cover in Syria from 2010 to 2018 using multitemporal Landsat imagery and GIS. *Land* **9**(7): 226. DOI: http://dx.doi.org/10.3390/land9070226.

Paulot, F, Jacob, DJ, Johnson, MT, Bell, TG, Baker, AR, Keene, WC, Lima, ID, Doney, SC, Stock, CA. 2015. Global oceanic emission of ammonia: Constraints from seawater and atmospheric observations. *Global Biogeochemical Cycles* **29**(8): 1165–1178. DOI: http://dx.doi.org/10.1002/2015GB005106.

Riddick, SN, Blackall, TD, Dragosits, U, Tang, YS, Moring, A, Daunt, F, Wanless, S, Hamer, KC, Sutton, MA. 2017. High temporal resolution modelling of environmentally-dependent seabird ammonia emissions: Description and testing of the GUANO model. *Atmospheric Environment* **161**: 48–60. DOI: http://dx.doi.org/10.1016/j.atmosenv.2017.04.020.

SANA. 2017, 21 Jul. Governmental delegation continues its visit to Homs, inspecting General Fertilizer Company. *Syrian Arab News Agency (SANA)*. Available at http://sana.sy/en/?p=110513. Accessed 23 March 2021.

Schlesinger, WH, Hartley, AE. 1992. A global budget for atmospheric NH_3. *Biogeochemistry* **15**(3): 191–211. DOI: http://dx.doi.org/10.1007/BF00002936.

Selby, J, Dahi, OS, Fröhlich, C, Hulme, M. 2017. Climate change and the Syrian civil war revisited. *Political Geography* **60**: 232–244. DOI: http://dx.doi.org/10.1016/j.polgeo.2017.05.007.

Sharpe, RR, Harper, LA. 1995. Soil, plant and atmospheric conditions as they relate to ammonia volatilization. *Fertilizer Research* **42**: 149–158.

Shephard, MW, Cady-Pereira, KE. 2015. Cross-track Infrared Sounder (CrIS) satellite observations of tropospheric ammonia. *Atmospheric Measurement Techniques* **8**(3): 1323–1336. DOI: http://dx.doi.org/10.5194/amt-8-1323-2015.

Sulla-Menashe, D, Friedl, MA. 2018. User guide to collection 6 MODIS land cover (MCD12Q1 and MCD12C1) product. Available at https://lpdaac.usgs.gov/documents/101/MCD12_User_Guide_V6.pdf.

Sulla-Menashe, D, Gray, JM, Abercrombie, SP, Friedl, MA. 2019. Hierarchical mapping of annual global land cover 2001 to present: The MODIS Collection 6 Land Cover product. *Remote Sensing of Environment* **222**: 183–194. DOI: http://dx.doi.org/10.1016/j.rse.2018.12.013.

The New Arab. 2019, 8 Apr. Russian military police beat Syrians following workers strike. *The New Arab*. Available at https://english.alaraby.co.uk/english/news/2019/4/8/russian-military-police-beat-syrians-following-workers-strike. Accessed 23 March 2021.

Theobald, MR, Crittenden, PD, Hunt, AP, Tang, YS, Dragosits, U, Sutton, MA. 2006. Ammonia emissions from a cape fur seal colony, Cape Cross, Namibia. *Geophysical Research Letters* **33**(3). DOI: http://dx.doi.org/10.1029/2005GL024384.

Tull, K. 2017. *Agriculture in Syria—K4D Helpdesk Report*. Brighton, UK: Institute of Development Studies. Available at https://opendocs.ids.ac.uk/opendocs/handle/20.500.12413/13081.

UNHCR. 2019. Forced displacement in 2019. Available at https://www.unhcr.org/be/wp-content/uploads/sites/46/2020/07/Global-Trends-Report-2019.pdf.

Van Damme, M, Clarisse, L, Franco, B, Sutton, MA, Erisman, JW, Kruit, RW, van Zanten, M, Whitburn, S, Hadji-Lazaro, J, Hurtmans, D, Clerbaux, C, Coheur, PF. 2021. Global, regional and national trends of atmospheric ammonia derived from a decadal (2008-2018) satellite record. *Environmental Research Letters* **16**: 055017. DOI: http://dx.doi.org/10.1088/1748-9326/abd5e0.

Van Damme, M, Clarisse, L, Whitburn, S, Hadji-Lazaro, J, Hurtmans, D, Clerbaux, C, Coheur, PF. 2018. Industrial and agricultural ammonia point sources exposed. *Nature* **564**(7734): 99–103. DOI: http://dx.doi.org/10.1038/s41586-018-0747-1.

Van Damme, M, Whitburn, S, Clarisse, L, Clerbaux, C, Hurtmans, D, Coheur, PF. 2017. Version 2 of the IASI NH_3 neural network retrieval algorithm; near-real

Downloaded from http://online.ucpress.edu/elementa/article-pdf/9/1/000041/483893/elementa.2021.000041.pdf by guest on 18 December 2021

time and reanalysed datasets. *Atmospheric Measurement Techniques Discussions*. DOI: http://dx.doi.org/10.5194/amt-2017-239.

Viatte, C, Petit, JE, Yamanouchi, S, Van Damme, M, Doucerain, C, Germain-Piaulenne, E, Gros, V, Favez, O, Clarisse, L, Coheur, PF, Strong, K, Clerbaux, C. 2021. Ammonia and $PM_{2.5}$ air pollution in Paris during the 2020 COVID lockdown. *Atmosphere* **12**(2): 160. DOI: http://dx.doi.org/10.3390/atmos12020160.

Viatte, C, Wang, T, Van Damme, M, Dammers, E, Meleux, F, Clarisse, L, Shephard, MW, Whitburn, S, Coheur, PF, Cady-Pereira, KE, Clerbaux, C. 2020. Atmospheric ammonia variability and link with particulate matter formation: A case study over the Paris area. *Atmospheric Chemistry and Physics* **20**(1): 577–596. DOI: http://dx.doi.org/10.5194/acp-20-577-2020.

Walsh, NP. 2014, 30 Dec. Life in the rubble of Kobani. *CNN*. Available at https://www.cnn.com/2014/12/04/world/meast/syria-kobani-civilians/index.html. Accessed 25 March 2021.

Washington Post. 2017, 3 Mar. Hezbollah, Russia and the U.S. help Syria retake Palmyra. *Washington Post*. Available at https://www.washingtonpost.com/world/syrian-army-retakes-the-ancient-city-of-palmyra-from-the-islamic-state/2017/03/02/fe770c78-ff63-11e6-9b78-824ccab94435_story.html. Accessed 24 March 2021.

Whitburn, S, Van Damme, M, Clarisse, L, Bauduin, S, Heald, CL, Hadji-Lazaro, J, Hurtmans, D, Zondlo, MA, Clerbaux, C, Coheur, PF. 2016. A flexible and robust neural network IASI-NH_3 retrieval algorithm. *Journal of Geophysical Research: Atmospheres* **121**(11): 6581–6599. DOI: http://dx.doi.org/10.1002/2016JD024828.

Whitburn, S, Van Damme, M, Kaiser, JW, van der Werf, GR, Turquety, S, Hurtmans, D, Clarisse, L, Clerbaux, C, Coheur, PF. 2015. Ammonia emissions in tropical biomass burning regions: Comparison between satellite-derived emissions and bottom-up fire inventories. *Atmospheric Environment* **121**: 42–54. DOI: http://dx.doi.org/10.1016/j.atmosenv.2015.03.015.

Wilson Center. 2019, 28 Oct. *Timeline: The rise, spread, and fall of the Islamic State*. Wilson Center. Available at https://www.wilsoncenter.org/article/timeline-the-rise-spread-and-fall-the-islamic-state.

Zammar, I, Kurita, H, Kii, A, Matsuo, N. 2006. Effective use of the waste gas emitted from ammonia production plant in Syria—Clean development mechanism - project design document form CDM PDD. Available at http://gec.jp/jpn/cdm-fs/2009/200918Shimiz_jSyria_pdd.pdf.

Zhu, L, Jacob, DJ, Mickley, LJ, Marais, EA, Cohan, DS, Yoshida, Y, Duncan, BN, González Abad, G, Chance, KV. 2014. Anthropogenic emissions of highly reactive volatile organic compounds in eastern Texas inferred from oversampling of satellite (OMI) measurements of HCHO columns. *Environmental Research Letters* **9**(11): 114004. DOI: http://dx.doi.org/10.1088/1748-9326/9/11/114004.

Downloaded from http://online.ucpress.edu/elementa/article-pdf/9/1/000041/483893/elementa.2021.000041.pdf by guest on 18 December 2021

How to cite this article: Abeed, R, Clerbaux, C, Clarisse, L, Van Damme, M, Coheur, P-F, Safieddine, S. 2021. A space view of agricultural and industrial changes during the Syrian civil war. *Elementa: Science of the Anthropocene* 9(1). DOI: https://doi.org/10.1525/elementa.2021.000041

Domain Editor-in-Chief: Detlev Helmig, Boulder AIR LLC, Boulder, CO, USA

Associate Editor: Paul Palmer, School of GeoSciences, The University of Edinburgh, Edinburgh, UK

Knowledge Domain: Atmospheric Science

Published: November 1, 2021 **Accepted:** October 9, 2021 **Submitted:** June 1, 2021

Copyright: © 2021 The Author(s). This is an open-access article distributed under the terms of the Creative Commons Attribution 4.0 International License (CC-BY 4.0), which permits unrestricted use, distribution, and reproduction in any medium, provided the original author and source are credited. See http://creativecommons.org/licenses/by/4.0/.

ELEMENTA Science of the Anthropocene

Elem Sci Anth is a peer-reviewed open access journal published by University of California Press.

OPEN ACCESS